Common neural choice signals emerge artifactually amidst multiple distinct value signals

Frömer, R.[1,3,4], Nassar, M.R.[2,3], Ehinger, B.V.[5], & Shenhav A.[1,3]

[1]Cognitive, Linguistic, and Psychological Sciences, [2]Department Neuroscience, [3]Carney Institute for Brain Sciences, Brown University, [4]University of Birmingham, Centre for Human Brain Health, School of Psychology, [5]University of Stuttgart, Stuttgart Center for Simulation Science

Classification: Social Sciences - Psychological and Cognitive Sciences

Keywords: decision-making, Appraisal, CPP, value

Correspondence should be addressed to Romy Frömer (r.froemer@bham.ac.uk)

Abstract

A large body of work has identified characteristic neural signatures of value-based decision-making. A core circuit has been shown to track the values of options under consideration, and the dynamics of neural activity associated with this circuit have been found to closely resemble the ramping evidence accumulation process believed to underpin goal-directed choice, most notably in the centroparietal positivity (CPP). However, recent neuroimaging studies suggest that value-based choices trigger multiple value-related neural signatures, some of which are unrelated to decision-making per se but instead reflect reflexive affective reactions to one's options. Here, we use the temporal resolution of EEG to test whether choice-independent value signals could be dissociated from well-known temporal signatures of the choice process. We show that EEG activity during value-based choice can be decomposed into distinct spatiotemporal clusters, one stimulus-locked (associated with the affective salience of a choice set) and one response-locked (associated with the difficulty of selecting the best option). We show that *neither* of these clusters meet the criteria for an evidence accumulation signal. Instead, and to our surprise, we find across two studies that stimulus-locked activity can *mimic* an evidence accumulation process when aligned to the response (as with the CPP). We then re-analyze four previous studies that demonstrate an evidence accumulation signal in the CPP – one during value-based decision-making, the others during perceptual decision-making – and show that this signal disappears when stimulus-locked and response-locked signals are jointly accounted for. Collectively, our findings show that neural signatures of value can reflect choice-independent processes that when analyzed using standard approaches, can look deceptively like evidence accumulation.

Significance Statement

To choose, people must evaluate their options and select between them. Selection is well described by a process of accumulating evidence up to some threshold, with an electrophysiological signature in the centroparietal positivity (CPP). However, decision-making also gives rise to value signals reflecting affective reactions and other selection-unrelated processes. Measuring EEG while participants made value-based choices, we identified two spatiotemporally distinct value signals, neither reflecting evidence accumulation. Instead, we show that evidence accumulation signals found in the CPP can arise artifactually from overlapping stimulus- and response-related activity. These findings call for a significant reexamination of established links between neural and computational mechanisms of choice, while inviting deeper consideration of the array of cognitive and affective processes that occur in parallel.

Over the past few decades, research has made significant advances toward understanding how people make value-based choices between competing options (e.g., items on a restaurant menu or in a store catalog). This research has identified consistent neural correlates of the values of the options under consideration (Bartra, McGuire, & Kable, 2013; Lebreton, Jorge, Michel, Thirion, & Pessiglione, 2009), and characterized the process that gives rise to decisions among them, both neurally and computationally (Hare, Schultz, Camerer, O'Doherty, & Rangel, 2011; Hunt, Kolling, Soltani, Woolrich, Rushworth, & Behrens, 2012; Pisauro, Fouragnan, Retzler, & Philiastides, 2017; Polania, Krajbich, Grueschow, & Ruff, 2014; Rangel & Hare, 2010). However, drawing clear links between neural and computational investigations of value-based choice has been complicated by the fact that neural correlates of value can reflect processes outside of the ongoing decision (for a review see Frömer & Shenhav, 2022). For instance, engaging with a choice set can trigger evaluations of one's options that are relatively automatic (e.g., Pavlovian) and potentially independent of the decision process itself (Daw, Niv, & Dayan, 2005; Frömer, Dean Wolf, & Shenhav, 2019; Grueschow, Polania, Hare, & Ruff, 2015; Guitart-Masip, Huys, Fuentemilla, Dayan, Duzel, & Dolan, 2012; Lebreton et al., 2009; Shenhav & Buckner, 2014; Shenhav, Dean Wolf, & Karmarkar, 2018; Shenhav & Karmarkar, 2019; van der Meer, Kurth-Nelson, & Redish, 2012). Distinguishing such choice-independent neural value signals from those that play a mechanistic role in the choice process requires disentangling the two types of signals within a measure of neural activity that provides the temporal resolution to uncover their unfolding dynamics. Here, we use EEG to explicitly tease apart value-based neural dynamics attributable to decision-making from those that are not, and reveal, surprisingly, that *only* the latter, choice-independent value signals were to be found.

Prevailing computational models show that decision-making can be described as a process of noisy evidence accumulating to a decision threshold, providing an account of choice behavior (choices and response times) across a variety of different choice settings (Ratcliff, Smith, Brown, & McKoon, 2016; Usher & McClelland, 2001). In the context of value-based decision-making, putative correlates of this evidence accumulation process have been identified throughout the brain (Hare et al., 2011; Hunt et al., 2012; Padoa-Schioppa & Conen, 2017; Pisauro et al., 2017) – often reflecting variability in the strength of evidence in favor of a particular option or attribute – and a subset of studies has used temporally-resolved estimates of neural activity to capture the dynamics of this evidence accumulation process. From this work, a putative EEG signature of evidence accumulation has emerged in the centroparietal positivity (CPP), both for perceptual (Kelly & O'Connell, 2013; O'Connell, Dockree, & Kelly, 2012; Twomey, Murphy, Kelly, & O'Connell, 2015) and value-based (Pisauro et al., 2017) choice. Researchers have shown that the CPP demonstrates three characteristic elements of evidence accumulation (cf. Fig 1A): (1) following stimulus presentation, activity is greater and peaks earlier when decision-related evidence is stronger (consistent with a more rapid rise of evidence accumulation when choices are easier), (2) activity peaks around the time of the response (consistent with a common response threshold), and (3) in the period leading up to the response, due to the slower accumulation and thus shallower slope, activity is greater when evidence is weaker and/or responses are slower. The latter effect is sometimes part of a cross-over pattern and complemented by an opposite effect at the time of response, reflecting perhaps a decrease in decision-threshold for longer RTs through an urgency signal or a modulation of the overlapping readiness potential (Gluth, Rieskamp, & Buchel, 2013; Kelly & O'Connell, 2013; Lui, Nunez, Cassidy, Vandekerckhove, Cramer, & Srinivasan, 2021), specifically in paradigms where there is

a clear on- and offset of the physical evidence (Kelly, Corbett, & O'Connell, 2021; Steinemann, O'Connell, & Kelly, 2018). The CPP is thus a potential index of value-based processing that is integral to decision-making per se.

However, recent studies have shown that neural correlates of choice value can reflect appraisals of the choice set as a whole, that take place irrespective of whether the participant is comparing their options (Frömer, Dean Wolf, & Shenhav, 2019; Shenhav & Karmarkar, 2019). For instance, using fMRI, dissociable components of the brain's valuation network (Bartra, McGuire, & Kable, 2013) were found to track how much participants liked a set of choice options overall versus elements of the choice process itself (e.g., whether they were engaged in choice versus appraisal, and how demanding the choice was; Shenhav & Buckner, 2014; Shenhav, Dean Wolf, & Karmarkar, 2018; Shenhav & Karmarkar, 2019). These studies suggest that value-related activity may emerge soon after the stimuli are presented that is tied to choice-independent, appraisal-like processes. They further predict that signatures of this appraisal process should be distinguishable from the evidence accumulation signatures described above, both in terms of the specific correlates of value that each of these tracks and, critically, in terms of their temporal dynamics (Fig 1A): whereas appraisal-related processes should index the overall value of a choice set, and occur transiently and locked to the presentation of the choice options; choice-related processes should index comparisons between one's options (e.g., the relative value of the chosen vs. unchosen option). The latter may reflect evidence accumulation, in which case such activity should ramp up between stimulus presentation and response selection (cf. Pisauro et al., 2017; Polania et al., 2014), or other choice-related processes (e.g. monitoring one's confidence). Past work has been unable to test these predictions because it lacked the temporal resolution needed to demonstrate these distinct temporal profiles and to formally tease

apart signals that meet the criteria of evidence accumulation from those that do not. As a result, it is unknown whether these value-related signals are indeed distinct or merely two components of a unitary choice process (Fig. 1A; cf. Hunt & Hayden, 2017; Hunt et al., 2012).

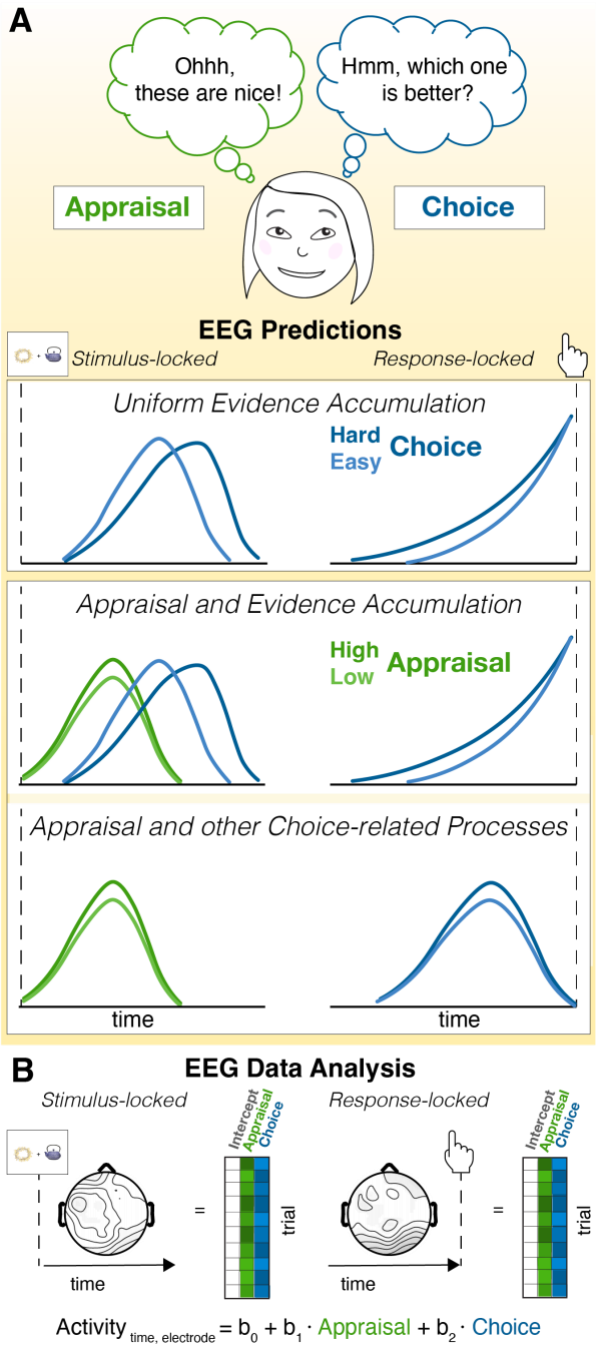

Figure 1. Dissociating appraisal- and choice-related processes. A. A set of options can elicit distinct evaluations, such as appraisal of the options and choice among them. Different frameworks make different predictions for whether and how those should affect neural activity locked to the response versus the stimulus. ***Top***: One account predicts that appraisal and choice reflect different temporal stages of a unitary evidence accumulation process, such that relevant variables (e.g., value similarity, blue) would be reflected first in stimulus-locked activity, and culminate at the time of the response. ***Middle/Bottom:*** Alternative accounts predict that appraisal reflects an *independent* process that emerges during stimulus presentation. Under these accounts, neural activity correlated with choice-related variables may emerge as a parallel process of evidence accumulation (i.e., both stimulus-locked and response-locked, **middle**) or in some other form as a non-accumulation-related signal (shown response-locked only as a stylized example- the shape and directionality of the signals may differ, **bottom**). **B.** To dissect the temporal dynamics of appraisal- and choice- related neural activity, we regress single trial EEG activity onto Appraisal-related and Choice -related variables (see Fig. 2C), separately

To fill this critical gap, we had participants make value-based decisions while undergoing EEG, and explicitly disentangled putative correlates of choice-independent appraisal processes (e.g., overall value and set liking) from correlates of the process of choice comparison (e.g., relative value and choice confidence). This allowed us to test two alternative hypotheses (Fig 1 A). One hypothesis is that value-related EEG activity would only emerge in the form of an evidence accumulation process, in which case we would expect any value-related variables (including overall value) to demonstrate characteristic patterns of stimulus-locked and response-locked activity previously observed, for instance, in the CPP (Fig 1 A top). The alternate hypothesis, motivated by our recent fMRI findings, is that we would observe appraisal-related patterns of activity that are selectively locked to stimulus presentation (reflecting their potentially more reflexive nature), independently of choice-related value signals. These choice-related value signals may take the form of CPP-like evidence accumulation signals (Fig 1 A middle), or some other form (Fig 1 A bottom).

We were able to rule out the first hypothesis, instead finding appraisal-related EEG activity that was both stimulus-locked and independent of choice comparison-related activity. Putatively choice-related EEG activity, by contrast, occurred in a distinct temporal window (response-locked) and with a different spatial profile (fronto-posterior) than the spatiotemporal cluster we identified for appraisal (stimulus-locked and parietal). Remarkably, these putative choice value signals *also* did not meet key criteria for an evidence accumulation signal. Instead, and even more striking, we found that such apparent evidence accumulation signals can emerge from *choice-independent* stimulus-locked activity, as an artifact of standard approaches to investigating evidence accumulation processes, due to bleed-over between stimulus-locked and response-locked activity (particularly for rapid choices). Confirming this, when we apply a novel

analysis approach that deconvolves stimulus and response-related activity to four previous decision-making studies, we eliminate signatures of evidence accumulation in the CPP previously observed in those data. As a result, our findings collectively, and unexpectedly, support a third hypothesis (Fig. 1A bottom): that value signals separately correlated with appraisal-related and choice-related processes emerge during value-based decision-making, but neither of these reflect evidence accumulation.

Results

We recorded EEG while participants made incentive-compatible choices between pairs of options (consumer goods). Choice sets varied in the overall and relative value of the two options, as determined by ratings of individual items given earlier in the session (Fig. 2A, B). Participants' choice behavior was consistent with that observed in previous studies and predicted by prevailing models of evidence accumulation (Pisauro et al., 2017; Polania et al., 2014; Ratcliff et al., 2016): participants chose faster (LMM fixed effect: $b = -348.7$ $p < .001$) and in a manner more accurate/consistent with their initial item ratings (GLMM fixed effect: $b = 4.54$, $p < .001$) as value difference increased, and also chose faster as overall value increased (LMM fixed effect: $b = 357.14$, $p < .001$; Fig. 2 B, Table S 1). After making all of their choices, participants provided subjective ratings of the choice sets (how much they liked the sets as a whole) and of the choices themselves (how much choice anxiety they had experienced while making the choice, and how confident they were in their final decision).

Distinct spatiotemporal clusters track indices of appraisal vs. choice comparison

We predicted that we would find a temporal dissociation between neural activity associated with appraisal versus choice, whereby appraisal-related activity would be temporally coupled with the onset of the stimuli whereas choice-related activity would be temporally

coupled with the response. To test this prediction, we analyzed the effects of appraisal and choice related variables on the same EEG data locked to the onset of the stimuli versus locked to the response. Given that a number of different variables captured our two constructs of interest - for instance, appraisal was captured by the overall (average) value of the choice set and subjective ratings of set liking, and choice was captured by the difference between the option values and subjective ratings of confidence (cf. Fig. 2B) - we used principal component analysis (PCA) to reduce the dimensionality of these single-trial measures and improve the robustness of our estimates of each construct.

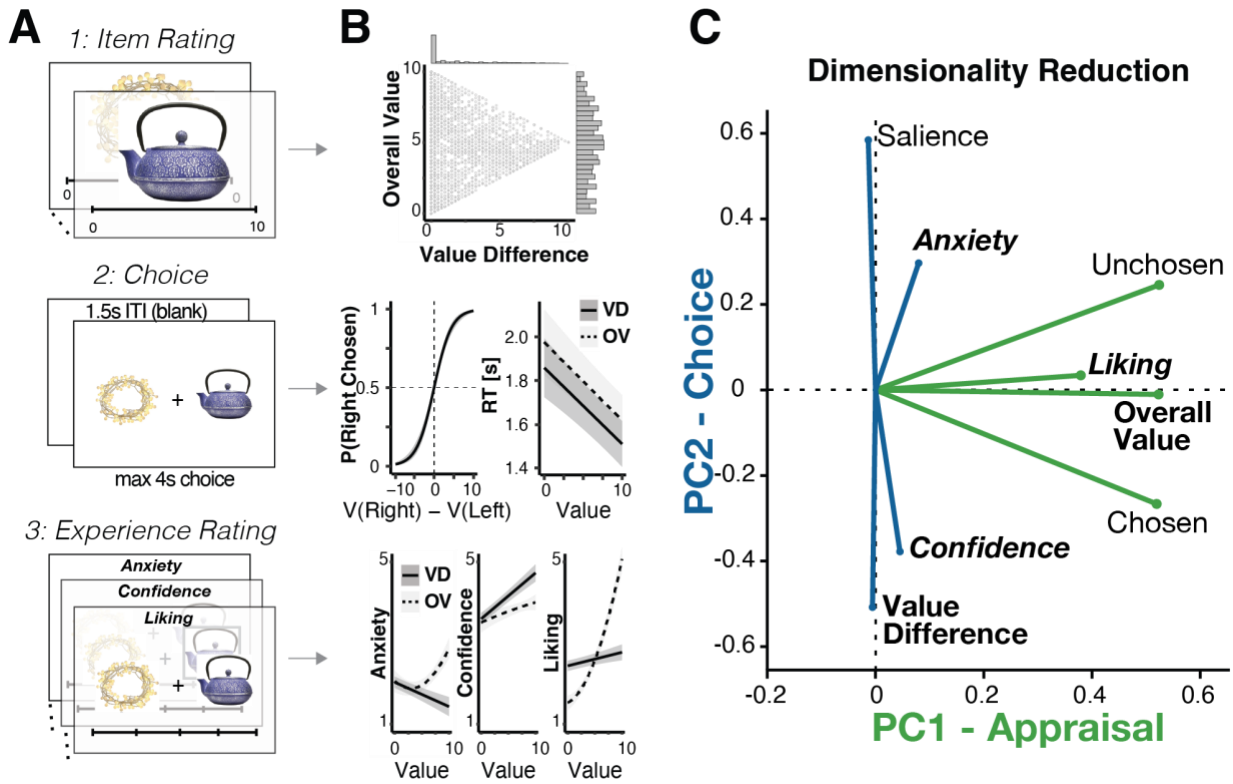

Figure 2. Integrating multiple measures of appraisal and choice. A. Participants performed the experiment in three phases, rating consumer goods individually (Phase 1) before choosing between pairs of those items (Phase 2) and finally rating their subjective experiences of those choices (Phase 3: set liking [appraisal], confidence, and anxiety). **B**. Responses across these phases provided different measures of appraisal and choice. ***Top:*** Option sets for Phase 2 were generated based on participants' initial item ratings to vary in their overall (average) value and the absolute difference between the values of the two options. ***Middle:*** Choices varied with the relative value of the chosen vs. unchosen option, and RTs varied with both overall value and value difference. ***Bottom:*** Overall value (OV; solid) and value difference

(VD; dotted) differentially influenced experiences of choice anxiety, confidence, and set liking. **C**. We used principal component analysis to reduce the dimensionality of our measures, identifying two principal components in our variable set, clustering naturally into variables associated with appraisal (PC1) versus choice (PC2). Component loadings for each measure are represented by their distance from the origin.

This PCA identified two reliable principal components (Fig. 2C, Table S2), one of which associated with how positively the option set had been assessed overall (e.g., positively loading on overall value and on ratings of choice set liking) and the other associated with how difficult the choice comparison was (e.g., negatively loading on value difference and on ratings of choice confidence). We termed these the Appraisal PC and Choice PC, respectively.

We regressed stimulus and response-locked single-trial EEG activity for each participant at each sensor and each time point onto these appraisal- and choice-related PCs (cf. Fig. 1 B), and identified significant stimulus- and response-related clusters associated with each PC using cluster-based permutation tests on the resulting t-statistics at the group level. We found that the PCs mapped onto distinct spatiotemporal patterns (Fig. 3, Supplementary Figure 1). In line with our predictions, we found that our Appraisal PC explained EEG activity locked to (and following) stimulus onset (Fig. 3A, $p = .040$, two-sided cluster permutation test, cf. Method), but not locked to the response (neither preceding nor following). The largest stimulus-locked cluster had a parietal distribution, peaking around 710 ms at CP2. Further in line with our hypothesis, we observed significant Choice PC-related activity locked to (and preceding) the response (Fig. 3B; $p = .002$ for a positive and $p < .001$ for the negative based on two-sided cluster-permutation tests), but not locked to and following the stimulus. The response-locked Choice PC activity included a frontocentral positive cluster, peaking around -566 ms at FC4, and a posterior negative cluster, peaking around -818 ms at P5. Similar clusters emerged when performing separate analyses on variables that constituted each of the PCs (Table S3).

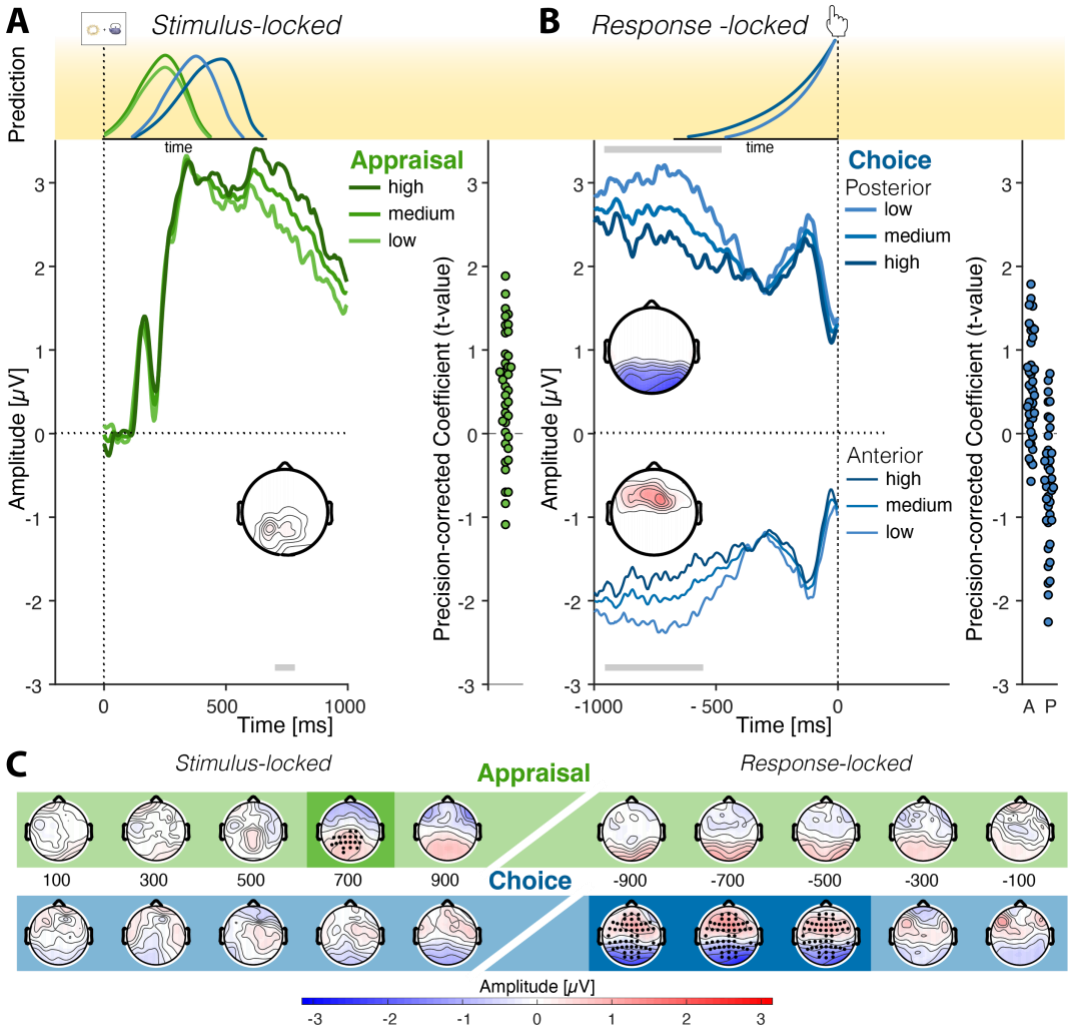

Figure 3. Appraisal and Choice exhibit dissociable spatio-temporal profiles. A – B. Curves show predicted ERPs for each level of a given PC from the regression model (visualized in discrete terciles), averaged within the electrodes in the respective cluster, within 1 second following stimulus onset (**A**) and preceding the response (**B**). Note that the median RT was approximately 1.7 s, so there is little overlap between stimulus- and response-locked data. Grey bars indicate cluster time points that significantly exceed permutation cluster masses (two-tailed test) for either the positive or negative clusters. Topographies display t-values within these clusters aggregated across cluster time points. To visualize the variability in the data underlying these clusters, individual participants' t-values are displayed on the right of each panel, aggregated within cluster times and electrodes. **A.** Stimulus-locked centroparietal positive activity increases with higher Appraisal PC scores (more positive appraisal). **B.** Response-locked posterior positivities and fronto-central negativities are reduced for higher Choice PC scores (more difficult trials). **C.** Coefficient topographies for the Appraisal PC (top) and Choice PC (bottom), averaged across sliding 200 ms windows aligned to stimulus (left) and response (right). Darker regions indicate time-windows encompassing significant clusters (cluster permutation corrected p <.05).

Neither value-related EEG signature is consistent with evidence accumulation

Our analyses suggest that two value-related EEG patterns emerge during value-based choice. The first of these was stimulus-locked, tracked appraisal-related measures (i.e., assessments of how much the participant liked the set overall), and had a timing and spatial distribution similar to that of the late positive potential (LPP), an ERP commonly found to index the affective salience of stimuli (Abdel Rahman, 2011; Schacht, Adler, Chen, Guo, & Sommer, 2012; Suess & Abdel Rahman, 2015), suggesting that this stimulus-locked cluster may index processes unrelated to the choice itself. By contrast, the response-locked value clusters we observed tracked measures of choice comparison (e.g., how much more valuable one option was than the other, and how certain the participant was in their choice), and had a spatiotemporal profile consistent with fronto-parietal EEG patterns that have been previously implicated in value-based decision-making (Polania et al., 2014; Polania, Moisa, Opitz, Grueschow, & Ruff, 2015). The posterior cluster overlapped topographically with the CPP (Kelly & O'Connell, 2013; O'Connell, Dockree, & Kelly, 2012; Pisauro et al., 2017; Twomey et al., 2015). We therefore reasoned that this response-locked cluster was a good candidate for providing an index of the evidence accumulation process leading up to the choice, and performed follow-up analyses to test whether activity in this or the more anterior cluster met the criteria for such a process.

Typically, evidence accumulation signals are also evident in stimulus-locked activity, because responses fully overlap with the stimulus time-window, leading to the characteristic greater and earlier peaks for faster evidence accumulation. Since in our study response times are longer, the absence of this pattern is expected. Surprisingly, however, neither of our response-locked clusters met the two response-locked criteria for signatures of evidence accumulation. First, rather than ramping towards a temporally common peak (marking the response threshold) immediately prior to a response, we found that activity peaked more than 500 ms prior to the

response. Second, rather than seeing greater activity leading up to a response on harder choice trials, reflecting the slower rate of evidence accumulation expected for those trials (compare light and dark lines in Fig. 3B), we instead found the opposite. Both frontal and posterior clusters showed greater amplitudes for easier as opposed to more difficult trials.

The fact that our data failed to meet either of these criteria was particularly notable for our posterior cluster, given its apparent overlap with the centroparietal positivity, the event-related potential most strongly associated with evidence accumulation. To better understand this discrepancy with previous work, we performed follow-up analyses focused directly on the CPP proper. Specifically, we tested for a key marker of evidence accumulation traditionally observed in the CPP: that slower trials (which require more evidence accumulation and exhibit a shallower slope) should show larger amplitudes leading up to the response than faster trials (Pisauro et al., 2017; Polania et al., 2014). In our study, CPP amplitudes in the pre-response time window (- 700 to -200 ms as in Pisauro et al., 2017) instead showed the opposite pattern: significantly larger for shorter relative to longer RTs (LMM fixed effect: b = - 0.47, t = -3.10, p = .002). Similar findings emerge when using value difference as a proxy for choice difficulty (as in the analyses above): CPP amplitude was larger for easier than harder choice trials (LMM fixed effect: b = 0.62, t = 1.77, p = .077) rather than the reverse.

One possible explanation for this apparent contradiction has to do with differences in the timing of choices in our study relative to previous studies. Our participants were given up to four seconds to make their choice, in contrast to shorter response windows in earlier work (e.g., 1.25s in Pisauro et al., 2017). The evidence accumulation signal may therefore have been more spread out in time within our data, leading the expected greater activity for slower/more difficult trials

to occur earlier. To investigate this possibility, we examined the average ERP curves on trials above and below the median RT (Fig 4 A).

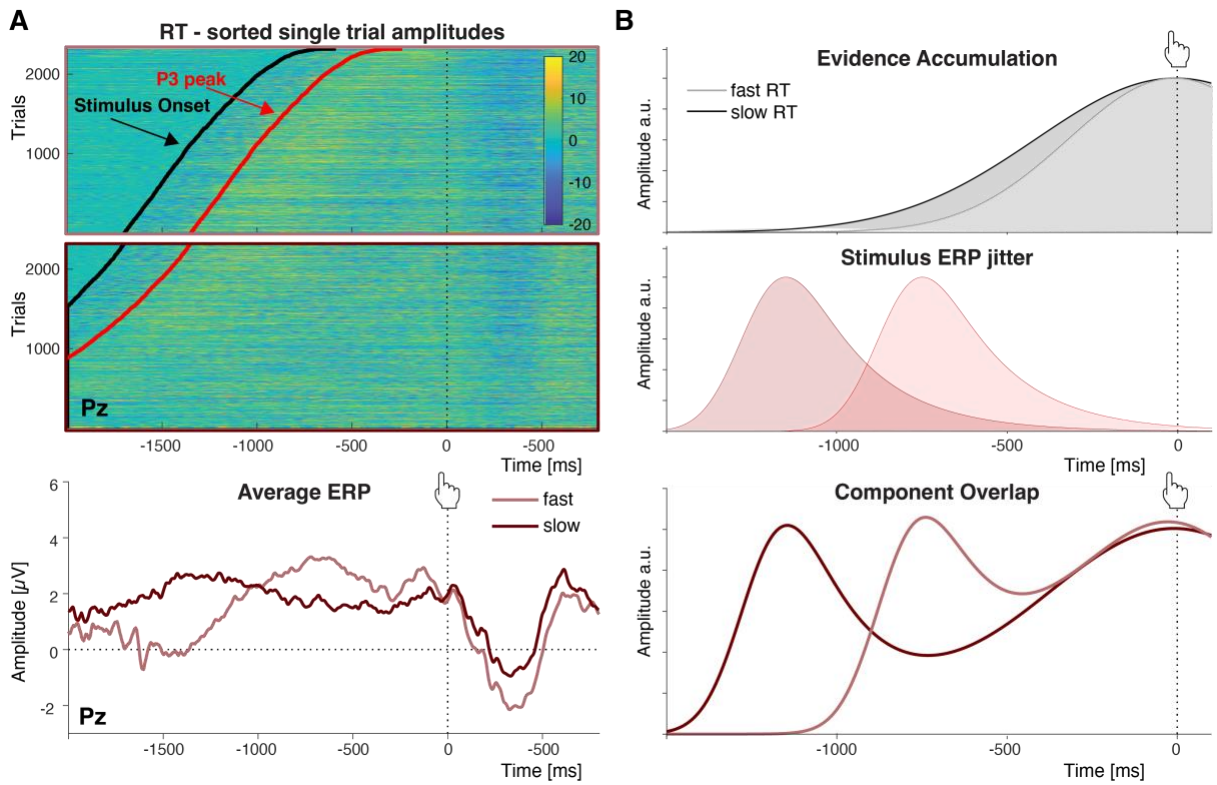

Figure 4. Stimulus-locked EEG activity can produce spurious patterns of response-locked activity due to variability in response times. A. ***Top:*** Response-locked single trial ERPs at Pz sorted by RT for trials faster (black box) and slower (grey box) than the median RT. Black lines mark stimulus onsets, and red lines mark the average onset of the stimulus-locked P3. ***Bottom:*** Averaging across these trials produces differential patterns of response-locked ERPs for faster trials (black) relative to slower trials (grey). **B.** The *unexpected* patterns observed in Panel A can result from component overlap. ***Top:*** Evidence accumulation signals expected for fast- and slow RTs respectively. ***Middle:*** When activity is locked to the response, this introduces jitter in stimulus-locked activity, with stimulus-related activity appearing earlier and earlier as RTs increase (i.e., the greater the delay between stimulus and response). ***Bottom:*** The convolution of the two patterns above can produce a pattern that is dominated by component overlap and obscures signatures of evidence accumulation. Such a pattern is similar to that shown in panel A.

Moving far enough back in time, to around 1s prior to response onset, we do see that the relative magnitudes of slow and fast trials reverses such that slow trials elicit greater activity than fast trials, as predicted by an evidence accumulation account. However, at odds with this account, we also see that slower trials elicit much *earlier* peaks than faster trials. To understand

why these peaks were systematically shifting in time, we plotted the single trial amplitudes underlying the median RT averages and sorted them by RT (Fig 4A top). This revealed a marked positive amplitude response in all trials (red line) approximately 350 ms following stimulus onset (black line), and the rise and peak of the ERP curves approximately followed the respective temporal distributions of this response (compare Fig 4 A top and bottom).

We therefore considered that the discrepancy between our findings and those previously observed (cf. Fig 4 B, top) may have been caused by overlap with this choice-unrelated response (Stimulus ERP jitter, Fig 4 B, middle) which may have masked the expected evidence accumulation signal. We therefore performed a separate analysis, analogous to standard event-related analyses for fMRI, which explicitly modeled stimulus-locked and response-locked activity, allowing them to be formally deconvolved from one another (Ehinger & Dimigen, 2019; Smith & Kutas, 2015a, 2015b). Like our previous analyses, this approach again identified a positive stimulus-locked appraisal cluster with a centro-parietal distribution (peak around 810 ms at electrode Pz, $p = .004$) and response-locked choice clusters over frontal (positive, peak around -722 ms at electrode AFz, $p = .010$) and parietal (negative, peak around -616 ms at electrode P8, $p = .010$) sites, respectively (Supplementary Figure 1, 2). This approach also showed no stimulus-locked choice effects, or response-locked appraisal effects. Thus, despite successfully disentangling the stimulus- and response-locked activity, it did not change our overall pattern of results; even after controlling for component overlap, our response-locked pattern remained inconsistent with evidence accumulation.

Evidence accumulation signals can emerge as an artifact of component overlap

These findings led us to question whether rather than *masking* evidence accumulation signals in our findings, stimulus-locked activity may have spuriously *caused* signatures of evidence accumulation in previous work. As we indicated earlier, most studies investigating evidence accumulation signals in EEG involved much faster decisions (~800ms on average in Kelly & O'Connell, 2013; ~1s on average in O'Connell, Dockree, & Kelly, 2012 except for a perturbation condition with additional stimulus dynamics; ~750ms on average in Pisauro et al., 2017; cf. Fig 5A). One possibility is therefore that the characteristic response-locked evidence accumulation pattern in prior studies was driven by overlap between *stimulus-related* activity (e.g., related to the salience of the stimuli) and response-locked activity (Smith & Kutas, 2015b). This *component overlap* account can explain basic features of CPP data, (Fig. 5A bottom) and makes a distinct prediction: rather than activity remaining locked to the response (as predicted by an evidence accumulation account), a component overlap account predicts that the peak of the CPP should move back in time as RTs increase (Fig. 5B bottom). As a consequence, for short-RTs, variability in the extent of overlap between stimulus-related and response-related activity with RT would produce an artifactual ramping signal in average ERPs that appears steeper for faster and shallower for slower responses. To test this possibility, we produced the same ERP plots as above for the subset of trials that had RTs shorter than 1.25 seconds, as in previous studies (Fig. 5B top). Compared to the entire dataset, the peaks for this subset of short RTs moved closer to the response and, crucially, a pattern reminiscent of the CPP emerged, with slower RT trials in this range displaying a larger parietal positivity up to 500 milliseconds prior to the response. Our collective pattern of results, across both short and long RTs, therefore exactly matches the predictions of the component overlap account (Fig. 5A/B bottom).

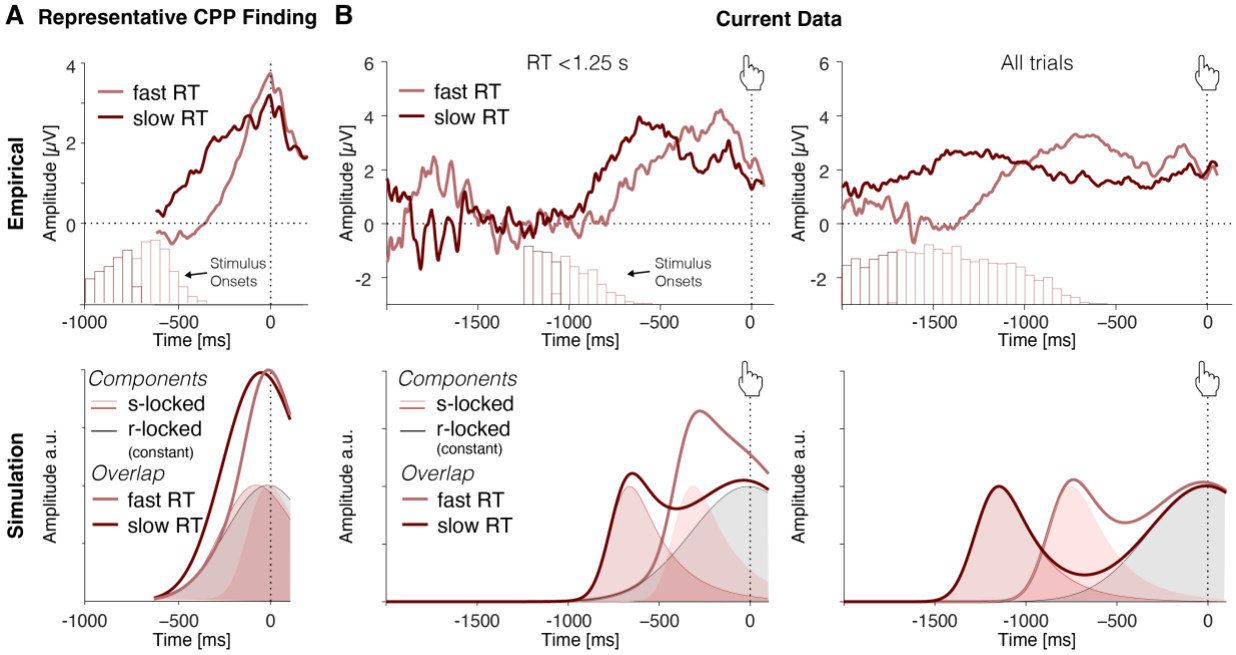

Figure 5. Evidence accumulation signals emerge as an artifact of component overlap. A. A representative CPP finding (data from Pisauro et al. 2017) shows faster ramping for ERPs curves from fast compared to slow trials. Histograms show distributions of stimulus onsets relative to the response for each average ERP curve. Simulation: Component overlap can generate an evidence accumulation-like pattern under plausible assumptions about RT distributions. Note that these simulations assume the same response-related component for all trials (black line), omitting any evidence accumulation. For fast response times (<900 ms on average), overlapping stimulus- and response-related component are predicted to resemble a single ramp-like component. The peak time and shape of the underlying component will depend on the mean and width of the RT distribution of trials in each ERP average. **B.** Data from our decision-making study are consistent with component overlap predictions. Shown are average ERPs for median split fast and slow RTs below 1.25 s (left) RT across all trials (right), respectively. Histograms show distributions of stimulus onsets relative to the response. Stimulus-evoked peaks move further away from the response as response times increase (top). Peak times and widths of the observed ERP curves vary with the mean and width of the RT distribution of the underlying trials. This pattern of results is consistent with a component overlap account (bottom).

To test whether these findings replicate in an independent sample, we examined the CPP in a separate value-based decision-making dataset (Study 2; N = 39) and found the same pattern: At odds with typical findings, CPP amplitudes in the pre-response time window (- 700 to -200 ms as in Pisauro et al., 2017) were again significantly larger for shorter relative to longer RTs (LMM fixed effect: b = - 1.01 t = -6.58, $p < .001$), and for easier than harder choice trials (LMM fixed effect: b = 0.87, t = 2.32, $p = .027$). When plotting fast and slow RT trials in a fast subset

of the data (RT < 1.25s) and across all trials as in Figure 5, we reproduce the moving peaks that follow the distribution of stimulus onsets (see Supplementary Figure 3).

However, it is still difficult to generalize from these results because in both studies our average RTs were longer than those in previous studies, even when only focusing on our subset of short-RT trials (those below 1.25s). As a result, rather than peaking exactly at the time of response (as is characteristic of past CPP results), EEG activity during that subset of trials peaks slightly before the response. To provide a more direct test of our hypothesis that the evidence accumulation effects in the CPP could originate from a component overlap artifact, we re-analyzed EEG findings from four previous datasets in which response times were more tightly constrained, one collected during value-based decision-making (Study 3; Pisauro et al., 2017) and the other three collected during perceptual decision-making (Boldt, Schiffer, Waszak, & Yeung, 2019; Frömer, Maier, & Abdel Rahman, 2018; Steinemann, O'Connell, & Kelly, 2018). In the value-based decision-making study, participants (N = 21) chose among pairs of snack items while their EEG was recorded and had to respond within 1.25s from stimulus onset. The authors found that behavior was well-captured with a DDM and reported the typical response-locked CPP evidence accumulation signal (cf. Fig. 4A top). In the first perceptual decision-making study (Study 4; Frömer, Maier, & Abdel Rahman, 2018), EEG was recorded while participants (N = 40) decided whether a deviant object in a circular array of objects was on the left or right side of the display (Fig 6). Objects in the array were chosen to be visually similar and presented either intact or blurred, which serves as an index of evidence strength and modulated performance accordingly (lower accuracy and slower RTs for blurred compared to intact stimuli). Stimuli were presented for 200 ms, and participants had up to 2 s from stimulus onset to respond. In the second perceptual decision-making study (Study 5; Steinemann,

O'Connell, & Kelly, 2018) EEG was recorded while participants (N = 17) determined which of two overlaid gratings had a higher contrast. Unlike the other studies, stimuli were not suddenly presented, but faded in at equal contrast and switched to the target contrasts after a random time interval simultaneously with a tone signaling the change. The evidence was then presented for 2400 ms within which participants had to respond. In the third perceptual decision-making dataset (Study 6; Boldt et al., 2019), EEG was recorded while participants (N = 17) judged the overall blueness versus redness of compound stimuli that varied in the blue, red and purple hue of their components. Stimuli were presented for 160ms and participants had 1200ms to decide.

When we separately reanalyze stimulus-locked and response-locked activity using mass-univariate analyses analogous to standard ERP analyses, we find the characteristic CPP indices of evidence accumulation over centroparietal sites in all four studies. Response-locked analyses revealed that activity peaked at the time of the response and rose with a steeper slope for fast relative to slow trials in value-based decision-making (Fig. 6A, top) and intact relative to blurred stimuli (Fig. 6B, top) and fast relative to slow trials (Fig. 6C-D, top) in perceptual decision-making, resulting in more positive CPP amplitudes for trials that putatively required more evidence accumulation, respectively (cf. Fig. 1A). The centro-parietal positivity in all studies therefore meets response-locked criteria for signatures of evidence accumulation. However, because these analyses do not explicitly account for the overlap between stimulus-related and response-related components, they cannot distinguish whether the response-locked patterns reflect evidence accumulation or stimulus-related activity. To formally disentangle these, we again applied the deconvolution approach introduced earlier (Ehinger & Dimigen, 2019), including stimulus and response events in a single model of neural responses. After deconvolution, we no longer find response-locked signatures of evidence accumulation in any of

the datasets (Fig. 6A-D, bottom), suggesting that this characteristic pattern of evidence accumulation only appeared in our previous analysis as an artifact of component overlap (see Supplementary Figure 4 for corresponding stimulus-locked activity).

So far, we assumed that non-decision time, comprising stimulus and motor processes at both ends of the evidence accumulation process, is constant, and that the time required for motor processes is short. However, some work suggests that both stimulus and motor processes can vary from trial to trial, leading to an evidence accumulation process that is not closely tied to either stimulus or response (Kelly, Corbett, & O'Connell, 2021). To test whether unfold's deconvolution approach would be robust to detecting evidence accumulation signals when accounting for these different forms of variability, we simulated the neurally informed DDM (simulation code adapted from Kelly & O'Connell) for strong and weak signals with varying ratios of stimulus and response variability. Indeed, as response variability increases, unfold will increasingly assign activity to the stimulus event, rather than the response event (Supplementary Figure 5). Importantly, these simulations show that any signatures of evidence accumulation are recoverable, either at the stimulus, the response, or both.

We had indeed observed a pattern in principle consistent with such stimulus-locked evidence accumulation signatures, but also with non-integration accounts, in the visual search dataset (Frömer, Maier, & Abdel Rahman, 2018), see Supplementary Figure 4B. To test whether signatures of evidence accumulation may have been moved towards the stimulus in the remaining datasets, and thus been missed in our previous analyses, we reanalyzed these data again, this time allowing stimulus-locked data to vary with response time in addition to allowing response-locked data to vary. The resulting patterns were not consistent with any of the simulated patterns (Supplementary Figure 6).

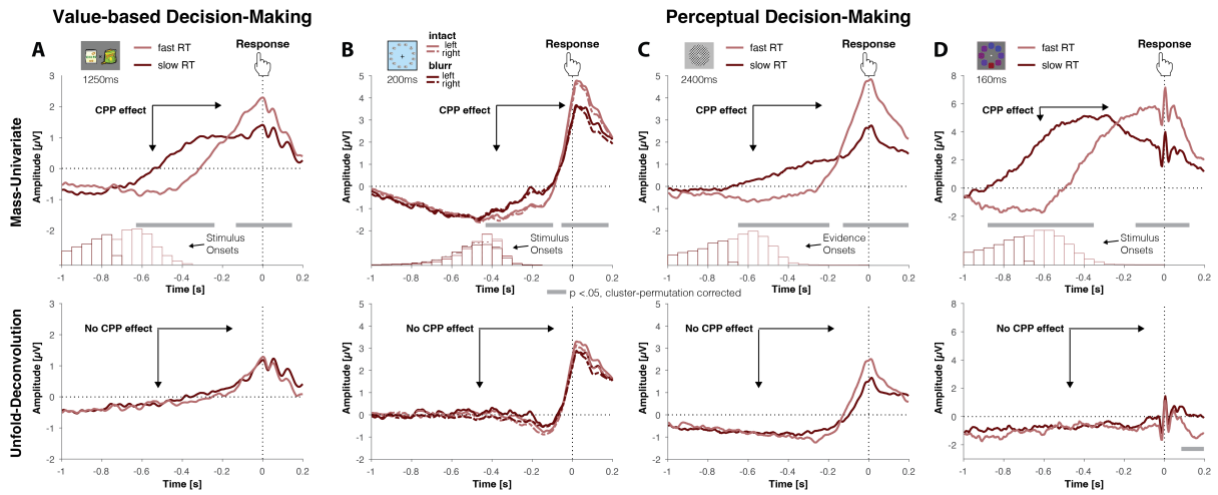

Figure 6. Response-locked evidence accumulation patterns vanish when correcting for component overlap. ***A.*** Regression ERPs (rERPs) from a mass-univariate re-analysis (top) of an independent value-based decision-making dataset (Pisauro, Fouragnan, Retzler, & Philiastides, 2017, cf Fig. 5A) exhibit a CPP with characteristic signatures of evidence accumulation. Decisions based on weaker evidence (slow compared to fast) are associated with a slower response-locked ramping of CPP amplitude, resulting in larger CPP amplitudes prior to the response. When re-analyzing these data with a deconvolution approach that models both stimulus-related and response-related activity (bottom), we find that response-locked rERPs no longer show the characteristic evidence accumulation pattern. **B - C.** Regression ERPs (rERPs) from a mass-univariate analysis (top) of three independent perceptual decision-making datasets exhibit a CPP with characteristic signatures of evidence accumulation. Decisions based on weaker evidence (blurred stimuli/slower responses) are associated with slower response-locked ramping of CPP amplitude, resulting in larger CPP amplitudes prior to the response. When re-analyzing these data with a deconvolution approach that models both stimulus-related and response-related activity (bottom), we find that response-locked rERPs no longer show the characteristic evidence accumulation pattern. Data are shown with average reference. **B.** Data from Frömer, Maier, & Abdel Rahman (2018). **C.** Data from Steinemann, O'Connell, & Kelly (2018). **D.** Data from Boldt, Schiffer, Waszak, & Yeung (2019). **A.-D.** Grey bars indicate temporal clusters significant at $p < .05$, cluster permutation-corrected for multiple comparisons.

Discussion

Previous work has identified reliable neural correlates of choice value, and interpreted them as elements of a uniform choice process in which option values are compared through an accumulation-to-bound process. These interpretations have been reinforced by evidence of such neural correlates ramping up towards the response, as would be expected of activity associated with evidence accumulation (Pisauro et al., 2017). However, recent work suggests that certain neural correlates of choice value are unrelated to goal-directed processes such as evidence

accumulation and instead reflect the appraisal of one's options (Frömer, Dean Wolf, & Shenhav, 2019; Shenhav & Buckner, 2014; Shenhav & Karmarkar, 2019). Here, we tested whether we could use EEG to temporally dissociate such choice-independent value signals from choice-related value signals. We anticipated that choice-independent value signals would follow shortly after stimulus onset, whereas choice-related activity should be coupled to and lead up to the response. We found this expected temporal dissociation. Remarkably, though, we found that choice-related activity was inconsistent with evidence accumulation, and that instead, putative signatures of evidence accumulation can emerge artifactually in standard response-locked analyses from overlapping stimulus-related activity. Across three value-based decision-making studies and three perceptual decision-making studies, we show that signatures of evidence accumulation are absent when stimulus-locked and response-locked activity are sufficiently separated in time, and disappear when overlapping activity is formally deconvolved.

It is important to note that our observation that correlates of appraisal (e.g., overall value) occur earlier in time than correlates of choice (e.g., value difference) does not in and of itself suggest that these signals arose from independent processes. Indeed, this same temporal pattern (overall value signals preceding value difference signals) is predicted to emerge from certain forms of unitary evidence accumulation processes, such as that of Wang and colleagues (Wang, 2002; Wong & Wang, 2006; see Hunt & Hayden, 2017; Hunt et al., 2012). However, models like this *also* predict that all these value signals should emerge locked to the response (Supplementary Figure 7). At odds with such an account, we only found stimulus-locked correlates of appraisal (unlike response-locked choice correlates). Our findings are thus better explained by *separate* mechanisms related to appraisal and choice.

The distinctiveness of these two sets of value signals is further supported by the fact that they were linked to distinct topographies. As predicted, we found appraisal-related activity temporally locked to stimulus onset - reflected in a parietal positivity consistent with an LPP ERP component (Abdel Rahman, 2011; Schacht et al., 2012; Suess & Abdel Rahman, 2015). The distribution and timing of this component parallels previous ERP findings on single item valuation (Harris, Adolphs, Camerer, & Rangel, 2011; Harris, Clithero, & Hutcherson, 2018), and therefore may be interpreted as reflecting an initial valuation stage prior to the onset of an independent choice comparison process (Lim, O'Doherty, & Rangel, 2011; Litt, Plassmann, Shiv, & Rangel, 2011; Plassmann, O'Doherty, & Rangel, 2010). Notably, the LPP is sensitive to affective information even when that information is not task relevant (Abdel Rahman, 2011; Bruchmann, Schindler, Heinemann, Moeck, & Straube, 2021) and its putative sources (Sun et al., 2017) overlap with the pregenual ACC and PCC regions in which we previously found choice-independent set appraisals (Shenhav & Karmarkar, 2019). Collectively, these findings suggest that rather than an initial choice-related valuation step, these appraisal-related signals reflect an automatic valuation signal (Lebreton, Abitbol, Daunizeau, & Pessiglione, 2015), or enhanced attention to such motivationally relevant events (Busch & VanRullen, 2010; Weichart, Turner, & Sederberg, 2020). Accordingly, we found that the variable that best predicted activity in our Appraisal Cluster was a participant's affective appraisal of the set (i.e., set liking, Table S2). Thus, appraisal-related activity may reflect initial (and perhaps reflexive) affective reactions to the stimuli (cf. Shenhav & Buckner, 2014; Shenhav & Karmarkar, 2019), and possibly serve to inform control decisions (Sun et al., 2017; Tajima, Drugowitsch, & Pouget, 2016) and/or future choices (Hall-McMaster, Dayan, & Schuck, 2021).

In contrast, choice-related activity was temporally locked to the response, and was characterized by a prominent frontocentral negativity and concomitant posterior positivity, consistent with previous findings demonstrating increased time-frequency coupling between frontoparietal regions, and stronger fronto-central beta power during value-based compared to perceptual decision-making (Polania et al., 2014; Polania et al., 2015). However, across two independent studies, follow-up analyses showed that this pattern of activity was inconsistent with it reflecting the *evidence accumulation* process leading up to the choice (Kelly & O'Connell, 2013; O'Connell, Dockree, & Kelly, 2012; Pisauro et al., 2017; Polania et al., 2014), in that amplitudes were larger for easier (or faster) rather than more difficult (or slower) trials. Thus, rather than merely constituting a negative result (i.e., lacking support for evidence accumulation reflected in the CPP), our results consistently *positively* contradict such predictions in favor of a different explanation. Our findings also rule out alternate versions of this evidence accumulation account whereby the decision threshold (or urgency signal) varies between decision-types with known differences in difficulty (Boldt et al., 2019) or over the course of the decision (Kelly, Corbett, & O'Connell, 2021). These varying-threshold accounts would still predict that activity would be locked to one's response, and are thus ruled out by the backward-shifting peaks we observed.

If these choice value correlates do not in fact reflect elements of the evidence accumulation process, what might they reflect? A prominent alternative account of such correlates would propose that signals associated with choice difficulty (e.g., value difference) that we observe in our choice clusters might instead reflect monitoring (e.g. conflict or confidence), which could inform higher-order decisions about further information sampling and potential information gain (Callaway, Rangel, & Griffiths, 2021; De Martino, Fleming, Garrett,

& Dolan, 2013; Desender, Boldt, & Yeung, 2018; Desender, Murphy, Boldt, Verguts, & Yeung, 2019; Hunt, 2021; Jang, Sharma, & Drugowitsch, 2021; Kaanders, Nili, O'Reilly, & Hunt, 2020; Kane, James, Shenhav, Daw, Cohen, & Aston-Jones, 2021; Lee & Daunizeau, 2019; Li, Nassar, Kable, & Gold, 2019; Monosov, 2020; Schulz, Fleming, & Dayan, 2021; Yeung & Summerfield, 2012). Recent work in value-based decision-making is converging on the idea that value based choice as studied here requires higher order decisions on gaze/attention allocation in the service of information sampling that fundamentally rely on representations of both value and uncertainty (Callaway, Rangel, & Griffiths, 2021; Gluth, Spektor, & Rieskamp, 2018; Hunt, 2021; Jang, Sharma, & Drugowitsch, 2021; Monosov, 2017, 2020; Sepulveda, Usher, Davies, Benson, Ortoleva, & De Martino, 2020; White et al., 2019). This functional interpretation is consistent with proposed loci of CPP activity in dACC (Pisauro et al., 2017), and decrements in choice consistency when fronto-central coupling is disrupted during value-based choice (Polania et al., 2015). While intriguing, this interpretation requires additional work to test specific predictions of a monitoring or active information search account.

Whatever the nature of these signals, our results call for caution when interpreting response-locked neural patterns as evidence accumulation. Across six datasets, we found that evidence accumulation signatures in the response-locked CPP may artificially arise from response time-dependent overlap with stimulus-related processing. This was true across both value-based and perceptual decision-making tasks. Considering the value-based decision-making studies only, one may have hypothesized that there is no CPP signature of value-based evidence accumulation, because the CPP is specific to perceptual evidence accumulation that precedes and is a necessary precursor to value-based evidence accumulation (cf. Frömer & Shenhav, 2022),

perhaps implemented through subcortical circuits. Yet, the collective findings of our reanalysis of three perceptual decision-making datasets speak against this hypothesis.

This is particularly notable since in their original analyses Steinemann, O'Connell, and Kelly (2018) had used a different algorithm (RIDE; Ouyang, Herzmann, Zhou, & Sommer, 2011) to subtract stimulus-locked activity associated with the auditory evidence onset cue and found the typical CPP patterns intact. This method separates early stimulus-locked components that are tightly temporally coupled from later activity that is not closely temporally coupled to the response, a central component. However, merely subtracting the stimulus-locked component determined this way does not offer information as to whether this central component is more aligned with the stimulus or the response, nor will it account for this component in response-locked analyses of the remaining data. If this central component occurred somewhat aligned to the stimulus, albeit more loosely than the early stimulus-locked activity, as a transient ERP, analyzing it locked to the response would still result in the same component overlap effect identified in this paper, and under certain conditions give the appearance of a ramp. Our findings suggest that the central component preserved in Steinemann, O'Connell, and Kelly (2018) is indeed locked to the stimulus as a canonical P3 ERP. This component is commonly observed for most behaviorally relevant visual stimuli, including feedback, regardless of response times, and is thought to potentially reflect a form of monitoring (Ullsperger, Fischer, Nigbur, & Endrass, 2014).

A crucial signature of evidence accumulation is that the corresponding signal peaks close to the time of the response, with that peak occurring earlier for faster compared to slower decisions. This is frequently observed for the CPP in perceptual decision making when the onset of the relevant stimulus is purposefully obscured, thus when the *subjective* onset of the stimulus

can vary relative to the *objective* onset (Kelly, Corbett, & O'Connell, 2021; Kelly, Corbett, & O'Connell, 2019; Kelly & O'Connell, 2013; Pereira et al., 2021). However, other decision-making studies that have identified the CPP as a signature of evidence accumulation only show response-locked activity (Boldt et al., 2019; Pisauro et al., 2017); and in some cases where stimulus-locked activity was examined, including our present results, the expected latency effect was not found (Sun et al., 2017). Our work highlights the importance of testing multiple predictions.

Doing so, several studies have shown that evidence accumulation signals simulated from diffusion model fits to behavior reproduce the CPP in detail, including its stimulus and response-aligned waveforms, the relationship between its pre-response amplitude and choice RT and accuracy and modulations of its pre-response amplitude by experimental manipulations of time pressure and prior knowledge (e.g., Kelly, Corbett, & O'Connell, 2021; O'Connell, Dockree, & Kelly, 2012; Twomey et al., 2015). Here, we highlight several cases in which such seemingly strong evidence could emerge artifactually from component overlap by virtue of evidence accumulation and component overlap sharing a common link to response time. Thus, in addition to testing multiple predictions of evidence accumulation accounts, future research can avoid misinterpretations of neural activity by inspecting ERP image plots for temporal patterns in single-trial data and deconvolving stimulus and response-locked signals (Ehinger & Dimigen, 2019) to show that the putative evidence accumulation pattern cannot be produced by component overlap alone.

While we have provided evidence for the pervasive risk that these artifacts pose for inferring evidence accumulation from the CPP, we can not claim to have definitively ruled out that the CPP can in certain cases carry the signature of an evidence accumulation signal. For

instance, one finding that is not easily accounted for by component overlap is O'Connell, Dockree, and Kelly's (2012) observation that perturbations in the stimulus lead to expected patterns in the CPP. In a continuous detection task, where participants needed to indicate when a stimulus was disappearing, O'Connell et al. showed that briefly increasing stimulus contrast led to an attenuation of the average stimulus-locked CPP that ramped up again as stimulus contrast continued to reduce. Such a pattern is difficult to explain with component overlap alone, but may still be accounted for by other non-integration accounts. Novel approaches are therefore needed to test the evidence accumulation hypothesis against alternative non-integration models (Latimer, Yates, Meister, Huk, & Pillow, 2015; Stine, Zylberberg, Ditterich, & Shadlen, 2020).

Our findings build on recent work in non-human animals, which has demonstrated that signatures of evidence accumulation can be necessary but not sufficient to conclude that a given neural population underpins the evidence accumulation process that drives choice. Using deactivation approaches, such studies have called into question the role of candidate regions of decision-making in parietal and prefrontal cortex that showed patterns expected for evidence accumulation using standard approaches (Erlich, Brunton, Duan, Hanks, & Brody, 2015; Hanks, Kopec, Brunton, Duan, Erlich, & Brody, 2015; Kane et al., 2021; Katz, Yates, Pillow, & Huk, 2016; but see also: Jeurissen, Shushruth, El-Shamayleh, Horwitz, & Shadlen, 2022). Similar to these findings, our work shows that evidence of accumulation is not sufficient to argue for an evidence accumulation account, and that to better understand the array of signals that appear over the course of a decision, we need to incorporate insights from affective science, metacognition and cognitive control (Frömer & Shenhav, 2022).

Method

Participants

For the main study 48 participants were recruited from Brown University and the general community. Of these 9 had to be excluded due to technical problems during data acquisition. The final sample consisted of 39 participants, (27 female) with a mean age of 20.84 years (SD = 3.90). Participants gave informed consent and received $10 per hour for their participation ($30 for the entire experiment). In addition to the compensation, participants could win one of their choices at the end of the experiment. The study was approved by Brown University's IRB.

The sample in study 2 comprised 39 participants recruited from Brown University and the general community. Participants (26 female, mean age 23.92, SD = 5.14), gave informed consent and received $10 or $15 per hour for their participation (the hourly rate as per IRB was increased after the study commenced and participants' payments were adjusted accordingly moving forward). This study was approved by Brown University's IRB, and not incentivized.

Please see the original publications for detailed participant information in Study 3 (N = 21; Pisauro et al., 2017), Study 4 (N = 40; Frömer, Maier, & Abdel Rahman, 2018), Study 5 (N = 17; Steinemann, O'Connell, & Kelly, 2018), and Study 6 (N= 17 after exclusion of 3 participants with non-matching behavioral and EEG data; Boldt et al., 2019).

Task and Procedure

The main experiment consisted of 3 parts: value rating, choice and subjective experience rating (Fig. 1A). The experimental procedure is an adapted version of that used in previous studies (Shenhav & Buckner, 2014; Shenhav & Karmarkar, 2019) to meet the requirements of EEG, specifically in the choice part.

In the first part, participants were presented with consumer goods, one at a time, and asked to rate how much they would like to have each of them on a continuous scale from 0 to 10 with zero being “not at all” and 10 being “a great deal”. Labels presented below each item supported their identification. Participants were encouraged to use the entire scale. Based on individual ratings, choice sets were created automatically, varying value difference and set value such that in half of the choices variance in value difference was maximized, while in the other half value difference was minimal and variance in set value was maximized (Shenhav, Dean Wolf, & Karmarkar, 2018).

In the second part, participants had to choose between two items presented left and right from a fixation cross by pressing the “A” or “L” key on a keyboard with their left or right index finger, respectively. At the beginning of the choice part, participants were placed at 90 cm distance to the screen with the keyboard in their lap and their fingers placed on the response keys. Images were presented with a size of 2° visual angle (115 pixel) each, at 1.3° visual angle (77 pixel) from a centrally presented fixation cross. Thus, the entire choice set extended to maximally 2.3° visual angle in each hemifield. This small stimulus size was chosen as to reduce eye movements by presenting the major portion of the stimuli foveally (radius of ~2 deg. visual angle; Strasburger, Rentschler, & Juttner, 2011). At the time of the response or after a maximum duration of 4s, the stimuli vanished from the screen and a fixation cross was presented for a constant 1.5 s inter trial interval. Before the beginning of the choice part, participants were informed that one of the choices would be randomly selected for a final gamble in the end of the experiment that would give them the opportunity to win the item they chose on that trial (N = 20 who won and received an item).

In the third part, participants were presented with all choices again to sequentially rate 1) their anxiety while making each particular choice, 2) their confidence in each choice, and 3) how much they liked each choice set, respectively. For all subjective evaluations the scales ranged from one to five mapped onto the corresponding number keys on the keyboard.

In the beginning and at the end of the experimental session, demographic and debrief data were collected, respectively, using Qualtrics. All subsequent parts were programmed in Psychophysics Toolbox (Brainard, 1997; Pelli, 1997) for Matlab (The MathWorks Inc.) and presented at 60 Hz on a 23 inch screen with a 1920 x 1080 resolution. Prior to the main experiment, participants filled in computerized personality questionnaires (Behavioral Inhibition/Activation Scales (BIS/BAS), Neuroticism subscale of the NEO Five Factor Inventory, Intolerance for Uncertainty Scale, and Need for Cognition). These data are not analyzed for the present study.

Study 2 differed in the following respects (cf. Frömer, Callaway, Griffiths, & Shenhav, 2022): Prior to the value ratings, participants viewed all items twice, once with labels and once without. During the second viewing they were asked to indicate whether they could recognize each item without seeing the label. During value ratings, participants for each item additionally evaluated their confidence in the value rating on a scale from 1 (not at all confident) to 5 (very confident). During the choice phase, rather than all at once, items were presented alternating individually at the center of the screen, until a decision was made, or 5 seconds elapsed while the duration of each item presentation was varied. One item was always presented longer on average than the other. Specific presentation durations on each turn were drawn from different distributions for long (M = 500 ms, SD = 100 ms) and short presentations (M = 200, SD = 50); these distributions were informed by previous work (Frömer & Shenhav, 2019). Response

buttons corresponding to each item were coded via blue and red colored frames around the options and manipulated independently of the order and duration of item presentation.

In Study 3 (Pisauro et al., 2017), participants chose among pairs of previously rated snack items and had to respond within 1.25s from stimulus onset. The difficulty of trials was manipulated by varying the value difference between options across 4 levels (1 through 4).

In Study 4 (Frömer, Maier, & Abdel Rahman, 2018), participants decided whether a deviant object in a circular array of objects was on the left or right side of the display. Objects in the array were chosen to be visually similar and presented either intact or blurred, which serves as an index of evidence strength and modulated performance accordingly (lower accuracy and slower RTs for blurred compared to intact stimuli). Stimuli were presented for 200 ms, and participants had up to 2 s from stimulus onset to respond.

In Study 5 (Steinemann, O'Connell, & Kelly, 2018), participants performed a contrast discrimination task in which they decided which of two overlaid grating patterns had a higher contrast. Participants were cued to either emphasize accuracy or speed and were rewarded when their responses met the current condition and punished when they did not. A trial began with a regimen cue, followed by neutral stimuli with equal contrast, which changed to the target stimulus alongside a tone to signal evidence onset and stayed on screen for 2400 ms. Participants received feedback following their response.

In Study 6 (Boldt et al., 2019), participants judged whether stimuli, each consistent of a circular array of 8 red, blue and purple circles, were more blue or more red on average. Across trials, the colored circles varied in their color strength (e.g., how clearly the stimulus was blue or red rather than purple) and in their variance (e.g., how variable the hues of the circles was). Stimuli were presented for 160 ms and participants had 1200 ms to respond. Participants were

cued to one of four conditions (high mean – low variance, low mean – low variance, high mean – high variance, low mean – high variance). They also provided prospective and retrospective confidence judgments.

Psychophysiological recording and processing

EEG data were recorded from 64 active electrodes (ActiCap, Brain Products, Munich, Germany) referenced against Cz with a sampling rate of 500 Hz using Brain Vision Recorder (Brain Products, Munich, Germany). Eye movements were recorded from electrodes placed at the outer canti (LO1, LO2) and below both eyes (IO1, IO2). Impedances were kept below 5 kΩ. EEG analyses were performed using customized Matlab (Versions 2017a and 2019b; The MathWorks Inc.) scripts and EEGLab (Version 13_6_5b; Delorme & Makeig, 2004) functions (cf. Frömer, Maier, & Abdel Rahman, 2018, for an earlier version of the pipeline). Offline data were re-referenced to average reference and corrected for ocular artifacts using brain electric source analyses (BESA; Ille, Berg, & Scherg, 2002) based on individual eye movements recorded after the experiment. The continuous EEG was low pass filtered at 40 Hz (eeglab FIR-filter, default filter coefficients). For mass-univariate analyses (see below), choice data was segmented into epochs of 4.2 s locked to stimulus onset, and 2.8 s relative to the response with 2 s pre- and 800 ms post response. Epochs were baseline-corrected to the 200 ms pre-stimulus interval for both segmentations. Trials containing artifacts (exceeding amplitude thresholds of +/-150µV or a gradient of 50µV) were excluded from further analyses. Unfold analyses were performed on unsegmented, preprocessed data as described below.

EEG data acquisition and processing for study 2 was identical except that passive Ag/Cl electrodes were used, and that segments were restricted to 2 s post stimulus and pre response, with 200ms pre stimulus and post response, respectively.

Please see the original publications for detailed information on EEG data acquisition in Study 3 (Pisauro et al., 2017), Study 4 (Frömer, Maier, & Abdel Rahman, 2018), Study 5 (Steinemann, O'Connell, & Kelly, 2018), and Study 6 (Boldt et al., 2019). We obtained preprocessed data for Studies 3 and 4. Raw data for Study 5 were concatenated across blocks, re-referenced and low-pass filtered at 40Hz. A subset of blocks (18 total from 298 blocks across all participants) could not be matched with the behavioral data and were excluded from further analyses. We obtained data for Study 6 with ocular artifact reduction and downsampled to 250Hz and removed horizontal and vertical EEG channels as well as M2. Data were then matched with behavioral data and low-pass filtered at 40Hz.

Analyses

Behavioral data were analyzed using linear mixed effects models as implemented in the lme4 package (Bates, Maechler, Bolker, & Walker, 2015) for R (Version 3.4.3; R Core Team, 2014). P-Values were computed using the sjplot package (Lüdecke, 2021). We modeled main effects for value variables (both fixed and random effects) in line with previous work (Frömer, Dean Wolf, & Shenhav, 2019; Hunt et al., 2012). Random effects components were removed if they explained no variance (Matuschek, Kliegl, Vasishth, Baayen, & Bates, 2017). Predictors in all analyses were mean centered, values were scaled to max equals 1 for ease of reporting. Choices were analyzed using generalized linear mixed effects models using a binomial link function with the dependent variable being probability of choosing the right item. In these cases, reported fixed effects are conditional on the random effects, because marginal fixed effects are difficult to estimate using Generalized Linear Mixed Models.

Appraisal and Choice principal components were derived from principal component analysis of all participants data on all trials on which a choice was made in time (4637/4680 trials) with the

following variables normalized to 0-1 ranges: chosen value (value of the item that was ultimately chosen), unchosen value (value of the item that was ultimately chosen), value difference (max value minus min value), overall value (average of both values), set salience (absolute mean centered overall value), anxiety, liking, and confidence. Thus, the dimensions of the input matrix were 4637 x 8. An initial exploratory PCA with permutation testing identified 2 principal components with eigenvalues greater than the 95th percentile than the distribution from shuffled data. We thus derived 2 principal components using matlab's pca function, rotated the factors (normalized varimax), and derived trial-wise scores by multiplying the trial indicators with the factor loadings. We thus reduced the variables above to one score for Appraisal and one for Choice for each trial.

EEG data were analyzed using a mass-univariate approach employing custom made Matlab scripts adapted from Collins and Frank (2016, 2018): For each subject, voltages at each electrode and time point (downsampled to 250 Hz) as dependent variables were regressed (using MATLAB's regress function which implements least squares regression) against trial parameters and an intercept term as independent variables to obtain regression weights for each predictor (similar to difference wave ERPs for each condition in traditional approaches, cf.: Smith & Kutas, 2015a). These regression weights were weighted by transforming them into t-values (dividing them by their standard error), effectively biasing unreliable estimates towards zero, and then submitted to group-level cluster-based permutation tests, employing a cluster forming threshold of $p = 0.005$. Clusters with masses (summed absolute t-values) larger than 2.5 % of the maximum cluster masses obtained from 1000 random permutation samples were considered significant. Observed cluster mass was compared to a permutation distribution to get a percentile rank, which was inverted (such that lower numbers corresponded to more unlikely events),

divided by 100 (to convert the percentile to a decimal), and multiplied by 2 to obtain a p-value for a two-sided test. We separately analyzed stimulus locked and response locked EEG data in the 1000 ms time interval following the stimulus and preceding the response, respectively. These time intervals were chosen in order to include sufficient trials at all time points. Data points outside the current trial range (following the response in stimulus-locked data and preceding the stimulus onset in response locked data) were set to nan to avoid spill-over from other trials or inter trial intervals. In the main analyses, the PC loadings for Appraisal and Choice PCs were included as independent variables with the intercept term. In three control analyses with the sets of variables underlying the PCs we entered as independent variables either overall value and value difference, Chosen and Unchosen Value, or Liking, Confidence and Anxiety alongside the intercept term.

For the deconvolution analyses, we conducted first level analyses on preprocessed data using the unfold toolbox (Ehinger & Dimigen, 2019). This MATLAB/Julia toolbox implements multiple regression with combined linear deconvolution for multivariate time-series similar to FIR-GLM analyses in fMRI. That is, by providing event-timings and per-event regression formulas, it allows us to disentangle temporally overlapping ERP responses (for detailed introduction to the method, see Ehinger & Dimigen, 2019; or Smith & Kutas, 2015b). Stimulus onsets and responses were modeled simultaneously with the same regressors as in the main analyses. Deconvolution was implemented using FIR/stick basis functions, time expanded +/- 2 seconds around the respective events. Artifacts (amplitudes exceeding +/- 250µV) were detected and removed using the built-in threshold functions. No baseline corrections were applied. The obtained betas were submitted to the same cluster-based permutation analyses for second level analyses as described above.

Study 4 perceptual decision-making data (Frömer, Maier, & Abdel Rahman, 2018) were analyzed using the same procedures as just described, except that we used +/-1 second time-windows due to the faster pace of the task, and additionally computed mass-univariate betas without overlap correction for comparison. The value-based decision-making data in Study 3 (Pisauro et al., 2017), as well as perceptual decision-making data in Studies 5 (Steinemann, O'Connell, & Kelly, 2018) and 6 (Boldt et al., 2019) were re-analyzed analogously using the Julia implementation of the unfold toolbox (Ehinger et al., 2023). Regressors for (Frömer, Maier, & Abdel Rahman, 2018) were visual field and stimulus quality, and both stimulus and response-locked activity were modeled with both regressors. Regressors for the three other studies were median split RT for response-locked activity, whereas we initially only modelled intercepts for stimulus locked activity. In a set of control analyses, we reanalyzed the data of the latter three studies to test whether stimulus and response-locked activity varied in ways predicted by unfold analyses of simulated data under different stimulus and response variability regimes.

Simulations. We simulated the neurally informed DDM based on code shared by Simon Kelly and Redmond O'Connell. In this model, stimulus processing as well as motor processes vary, so that the timing of the evidence accumulation process in between both is jittered. Both jitters were modelled using the simplifying assumption of uniform distributions with duration "stim_jitter" and "motor_jitter", respectively. Further, we report the ratio stim_jitter/motor_jitter, indicating whether the evidence accumulation process is more closely associated with the stimulus or the motor. We simulated 3 scenarios, 1) 2/1 ratio, whereby stim_jitter was set to 0.2s and motor_jitter to 0.1s, 2) 1/1 ratio, where both were set to 0.2s, and 3) 1/2 ratio, where stim_jitter was set to 0.1s and motor_jitter to 0.2s.

Acknowledgments

This work was funded by a Center of Biomedical Research Excellence grant P20GM103645 from the National Institute of General Medical Sciences (A.S.), grant R01MH124849 from the National Institute of Mental Health (A.S.), and by the Deutsche Forschungsgemeinschaft (DFG, German Research Foundation) under Germany´s Excellence Strategy – EXC 2075 – 390740016 (B.V.E.). The authors are grateful to Wasita Mahaphanit, Cornelius Braun, and Hattie Xu for assistance in data collection, Kerstin Unger, Andrea Mueller and Dan McCarthy for support with the EEG setup, Avinash Vaidya for generously sharing code and advice, to Andrea Pisauro et al., Natalie Steinemann et al, and Annika Boldt et al., for sharing their data, additional information for their reanalysis, and thoughtful questions, and to Rafael Polania, and Michael J. Frank for helpful discussion, and to Simon Kelly and Redmond O'Connell for extensive, fruitful discussions and for sharing their simulation code.

Data Availability

Data for Studies 1, 3 and 4 are available through on different platforms with links provided through github under: https://github.com/froemero/Common_Neural_Choice_Signals_emerge_artifactually. Data for Study 2 will be made available upon publication of the primary results not reported here.

Code Availability

All code can be accessed under https://github.com/froemero/Common_Neural_Choice_Signals_emerge_artifactually.

References

Abdel Rahman, R. (2011). Facing good and evil: Early brain signatures of affective biographical knowledge in face recognition. *Emotion, 11*(6), 1397-1405. doi:10.1037/a0024717

Bartra, O., McGuire, J. T., & Kable, J. W. (2013). The valuation system: A coordinate-based meta-analysis of BOLD fMRI experiments examining neural correlates of subjective value. *Neuroimage, 76*, 412-427. doi:https://doi.org/10.1016/j.neuroimage.2013.02.063

Bates, D., Maechler, M., Bolker, B. M., & Walker, S. C. (2015). Fitting Linear Mixed-Effects Models Using lme4. *Journal of Statistical Software, 67*(1), 1-48. Retrieved from <Go to ISI>://WOS:000365981400001

Boldt, A., Schiffer, A.-M., Waszak, F., & Yeung, N. (2019). Confidence Predictions Affect Performance Confidence and Neural Preparation in Perceptual Decision Making. *Scientific Reports, 9*(1), 4031. doi:10.1038/s41598-019-40681-9

Brainard, D. H. (1997). The Psychophysics Toolbox. *Spat Vis, 10*(4), 433-436.

Bruchmann, M., Schindler, S., Heinemann, J., Moeck, R., & Straube, T. (2021). Increased early and late neuronal responses to aversively conditioned faces across different attentional conditions. *Cortex, 142*, 332-341. doi:10.1016/j.cortex.2021.07.003

Busch, N. A., & VanRullen, R. (2010). Spontaneous EEG oscillations reveal periodic sampling of visual attention. *Proc Natl Acad Sci U S A, 107*(37), 16048-16053. doi:10.1073/pnas.1004801107

Callaway, F., Rangel, A., & Griffiths, T. L. (2021). Fixation patterns in simple choice reflect optimal information sampling. *Plos Computational Biology, 17*(3), e1008863. doi:10.1371/journal.pcbi.1008863

Collins, A. G. E., & Frank, M. J. (2016). Neural signature of hierarchically structured expectations predicts clustering and transfer of rule sets in reinforcement learning. *Cognition, 152*, 160-169. doi:10.1016/j.cognition.2016.04.002

Collins, A. G. E., & Frank, M. J. (2018). Within- and across-trial dynamics of human EEG reveal cooperative interplay between reinforcement learning and working memory. *Proc Natl Acad Sci U S A, 115*(10), 2502-2507. doi:10.1073/pnas.1720963115

Daw, N. D., Niv, Y., & Dayan, P. (2005). Uncertainty-based competition between prefrontal and dorsolateral striatal systems for behavioral control. *Nat Neurosci, 8*(12), 1704-1711. doi:10.1038/nn1560

De Martino, B., Fleming, S. M., Garrett, N., & Dolan, R. J. (2013). Confidence in value-based choice. *Nat Neurosci, 16*(1), 105-110. doi:10.1038/nn.3279

Delorme, A., & Makeig, S. (2004). EEGLAB: an open source toolbox for analysis of single-trial EEG dynamics including independent component analysis. *J Neurosci Methods, 134*(1), 9-21. doi:10.1016/j.jneumeth.2003.10.009

Desender, K., Boldt, A., & Yeung, N. (2018). Subjective Confidence Predicts Information Seeking in Decision Making. *Psychol Sci, 0*(0), 956797617744771. doi:10.1177/0956797617744771

Desender, K., Murphy, P., Boldt, A., Verguts, T., & Yeung, N. (2019). A post-decisional neural marker of confidence predicts information-seeking in decision-making. *Journal of Neuroscience*, 2620-2618. doi:10.1523/JNEUROSCI.2620-18.2019

Ehinger, B. V., Alday, P. M., Schepers, J., Kleinschmidt, D., Skukies, R., Mikheev, V., & Yehudi, Y. (2023). Unfold.jl (Version 0.4.1).

Ehinger, B. V., & Dimigen, O. (2019). Unfold: an integrated toolbox for overlap correction, non-linear modeling, and regression-based EEG analysis. *PeerJ, 7*, e7838. doi:10.7717/peerj.7838

Erlich, J. C., Brunton, B. W., Duan, C. A., Hanks, T. D., & Brody, C. D. (2015). Distinct effects of prefrontal and parietal cortex inactivations on an accumulation of evidence task in the rat. *Elife, 4*, e05457. doi:10.7554/eLife.05457

Frömer, R., Callaway, F., Griffiths, T., & Shenhav, A. (2022). Considering what we know and what we don't know: Expectations and Confidence guide value integration in value-based decision-making. *PsyArXiv*. doi:10.31234/osf.io/2sqyt

Frömer, R., Dean Wolf, C. K., & Shenhav, A. (2019). Goal congruency dominates reward value in accounting for behavioral and neural correlates of value-based decision-making. *Nature Communications, 10*(1), 4926. doi:10.1038/s41467-019-12931-x

Frömer, R., Maier, M., & Abdel Rahman, R. (2018). Group-Level EEG-Processing Pipeline for Flexible Single Trial-Based Analyses Including Linear Mixed Models. *Front Neurosci, 12*(48). doi:10.3389/fnins.2018.00048

Frömer, R., & Shenhav, A. (2019). Spatiotemporally distinct neural mechanisms underlie our reactions to and comparison between value-based options. *bioRxiv*, 609198. doi:10.1101/609198

Frömer, R., & Shenhav, A. (2022). Filling the gaps: Cognitive control as a critical lens for understanding mechanisms of value-based decision-making. *Neuroscience & Biobehavioral Reviews, 134*, 104483. doi:https://doi.org/10.1016/j.neubiorev.2021.12.006

Gluth, S., Rieskamp, J., & Buchel, C. (2013). Classic EEG motor potentials track the emergence of value-based decisions. *Neuroimage, 79*, 394-403. doi:10.1016/j.neuroimage.2013.05.005

Gluth, S., Spektor, M. S., & Rieskamp, J. (2018). Value-based attentional capture affects multi-alternative decision making. *Elife, 7*, e39659. doi:10.7554/eLife.39659

Grueschow, M., Polania, R., Hare, Todd A., & Ruff, Christian C. (2015). Automatic versus Choice-Dependent Value Representations in the Human Brain. *Neuron, 85*(4), 874-885. doi:10.1016/j.neuron.2014.12.054

Guitart-Masip, M., Huys, Q. J., Fuentemilla, L., Dayan, P., Duzel, E., & Dolan, R. J. (2012). Go and no-go learning in reward and punishment: interactions between affect and effect. *Neuroimage, 62*(1), 154-166. doi:10.1016/j.neuroimage.2012.04.024

Hall-McMaster, S., Dayan, P., & Schuck, N. W. (2021). Control over patch encounters changes foraging behaviour. *bioRxiv*, 2021.2001.2019.426950. doi:10.1101/2021.01.19.426950

Hanks, T. D., Kopec, C. D., Brunton, B. W., Duan, C. A., Erlich, J. C., & Brody, C. D. (2015). Distinct relationships of parietal and prefrontal cortices to evidence accumulation. *Nature, 520*(7546), 220-223. doi:10.1038/nature14066

Hare, T. A., Schultz, W., Camerer, C. F., O'Doherty, J. P., & Rangel, A. (2011). Transformation of stimulus value signals into motor commands during simple choice. *Proc Natl Acad Sci U S A, 108*(44), 18120-18125. doi:10.1073/pnas.1109322108

Harris, A., Adolphs, R., Camerer, C., & Rangel, A. (2011). Dynamic construction of stimulus values in the ventromedial prefrontal cortex. *PLoS One, 6*(6), e21074. doi:10.1371/journal.pone.0021074

Harris, A., Clithero, J. A., & Hutcherson, C. A. (2018). Accounting for Taste: A Multi-Attribute Neurocomputational Model Explains the Neural Dynamics of Choices for Self and Others. *Journal of Neuroscience, 38*(37), 7952-7968. doi:10.1523/JNEUROSCI.3327-17.2018

Hunt, L. T. (2021). Frontal circuit specialisations for decision making. *Eur J Neurosci, 53*(11), 3654-3671. doi:10.1111/ejn.15236

Hunt, L. T., & Hayden, B. Y. (2017). A distributed, hierarchical and recurrent framework for reward-based choice. *Nat Rev Neurosci, 18*(3), 172-182. doi:10.1038/nrn.2017.7

Hunt, L. T., Kolling, N., Soltani, A., Woolrich, M. W., Rushworth, M. F., & Behrens, T. E. (2012). Mechanisms underlying cortical activity during value-guided choice. *Nat Neurosci, 15*(3), 470-476, S471-473. doi:10.1038/nn.3017

Ille, N., Berg, P., & Scherg, M. (2002). Artifact correction of the ongoing EEG using spatial filters based on artifact and brain signal topographies. *Journal of Clinical Neurophysiology, 19*(2), 113-124. doi:10.1097/00004691-200203000-00002

Jang, A. I., Sharma, R., & Drugowitsch, J. (2021). Optimal policy for attention-modulated decisions explains human fixation behavior. *Elife, 10*, e63436. doi:10.7554/eLife.63436

Jeurissen, D., Shushruth, S., El-Shamayleh, Y., Horwitz, G. D., & Shadlen, M. N. (2022). Deficits in decision-making induced by parietal cortex inactivation are compensated at two timescales. *Neuron*. doi:10.1016/j.neuron.2022.03.022

Kaanders, P., Nili, H., O'Reilly, J. X., & Hunt, L. T. (2020). Medial frontal cortex activity predicts information sampling in economic choice. *bioRxiv*, 2020.2011.2024.395814. doi:10.1101/2020.11.24.395814

Kane, G. A., James, M. H., Shenhav, A., Daw, N. D., Cohen, J. D., & Aston-Jones, G. (2021). Rat Anterior Cingulate Cortex Continuously Signals Decision Variables in a Patch Foraging Task. *bioRxiv*, 2021.2006.2007.447464. doi:10.1101/2021.06.07.447464

Katz, L. N., Yates, J. L., Pillow, J. W., & Huk, A. C. (2016). Dissociated functional significance of decision-related activity in the primate dorsal stream. *Nature, 535*(7611), 285-288. doi:10.1038/nature18617

Kelly, S. P., Corbett, E. A., & O'Connell, R. G. (2021). Neurocomputational mechanisms of prior-informed perceptual decision-making in humans. *Nat Hum Behav, 5*(4), 467-481. doi:10.1038/s41562-020-00967-9

Kelly, S. P., Corbett, E. A., & O'Connell, R. G. (2019). Multifaceted adaptation of the neural decision process with prior knowledge of time constraints and stimulus probability. *bioRxiv*, 715318. doi:10.1101/715318

Kelly, S. P., & O'Connell, R. G. (2013). Internal and external influences on the rate of sensory evidence accumulation in the human brain. *J Neurosci, 33*(50), 19434-19441. doi:10.1523/JNEUROSCI.3355-13.2013

Latimer, K. W., Yates, J. L., Meister, M. L., Huk, A. C., & Pillow, J. W. (2015). Single-trial spike trains in parietal cortex reveal discrete steps during decision-making. *Science, 349*(6244), 184-187. doi:10.1126/science.aaa4056

Lebreton, M., Abitbol, R., Daunizeau, J., & Pessiglione, M. (2015). Automatic integration of confidence in the brain valuation signal. *nature neuroscience, 18*, 1159. doi:10.1038/nn.4064

https://www.nature.com/articles/nn.4064#supplementary-information

Lebreton, M., Jorge, S., Michel, V., Thirion, B., & Pessiglione, M. (2009). An automatic valuation system in the human brain: evidence from functional neuroimaging. *Neuron, 64*(3), 431-439. doi:10.1016/j.neuron.2009.09.040

Lee, D., & Daunizeau, J. (2019). Trading Mental Effort for Confidence: The Metacognitive Control of Value-Based Decision-Making. *bioRxiv*, 837054. doi:10.1101/837054

Li, Y. S., Nassar, M. R., Kable, J. W., & Gold, J. I. (2019). Individual Neurons in the Cingulate Cortex Encode Action Monitoring, Not Selection, during Adaptive Decision-Making. *Journal of Neuroscience, 39*(34), 6668-6683. doi:10.1523/JNEUROSCI.0159-19.2019

Lim, S.-L., O'Doherty, J. P., & Rangel, A. (2011). The Decision Value Computations in the vmPFC and Striatum Use a Relative Value Code That is Guided by Visual Attention. *The Journal of Neuroscience, 31*(37), 13214-13223. doi:10.1523/jneurosci.1246-11.2011

Litt, A., Plassmann, H., Shiv, B., & Rangel, A. (2011). Dissociating valuation and saliency signals during decision-making. *Cerebral Cortex, 21*(1), 95-102. doi:10.1093/cercor/bhq065

Lüdecke, D. (2021). sjPlot: Data Visualization for Statistics in Social Science. Retrieved from https://CRAN.R-project.org/package=sjPlot

Lui, K. K., Nunez, M. D., Cassidy, J. M., Vandekerckhove, J., Cramer, S. C., & Srinivasan, R. (2021). Timing of Readiness Potentials Reflect a Decision-making Process in the Human Brain. *Computational Brain & Behavior, 4*(3), 264-283. doi:10.1007/s42113-020-00097-5

Matuschek, H., Kliegl, R., Vasishth, S., Baayen, H., & Bates, D. (2017). Balancing Type I error and power in linear mixed models. *Journal of Memory and Language, 94*, 305-315. doi:10.1016/j.jml.2017.01.001

Monosov, I. E. (2017). Anterior cingulate is a source of valence-specific information about value and uncertainty. *Nature Communications, 8*(1), 134. doi:10.1038/s41467-017-00072-y

Monosov, I. E. (2020). How Outcome Uncertainty Mediates Attention, Learning, and Decision-Making. *Trends in Neurosciences*. doi:10.1016/j.tins.2020.06.009

O'Connell, R. G., Dockree, P. M., & Kelly, S. P. (2012). A supramodal accumulation-to-bound signal that determines perceptual decisions in humans. *nature neuroscience, 15*(12), 1729-+. doi:10.1038/nn.3248

Ouyang, G., Herzmann, G., Zhou, C., & Sommer, W. (2011). Residue iteration decomposition (RIDE): A new method to separate ERP components on the basis of latency variability in single trials. *Psychophysiology, 48*(12), 1631-1647. doi:10.1111/j.1469-8986.2011.01269.x

Padoa-Schioppa, C., & Conen, K. E. (2017). Orbitofrontal Cortex: A Neural Circuit for Economic Decisions. *Neuron, 96*(4), 736-754. doi:10.1016/j.neuron.2017.09.031

Pelli, D. G. (1997). The VideoToolbox software for visual psychophysics: transforming numbers into movies. *Spat Vis, 10*(4), 437-442.

Pereira, M., Megevand, P., Tan, M. X., Chang, W., Wang, S., Rezai, A., . . . Faivre, N. (2021). Evidence accumulation relates to perceptual consciousness and monitoring. *Nat Commun, 12*(1), 3261. doi:10.1038/s41467-021-23540-y

Pisauro, M. A., Fouragnan, E., Retzler, C., & Philiastides, M. G. (2017). Neural correlates of evidence accumulation during value-based decisions revealed via simultaneous EEG-fMRI. *Nat Commun, 8*, 15808. doi:10.1038/ncomms15808

Plassmann, H., O'Doherty, J. P., & Rangel, A. (2010). Appetitive and aversive goal values are encoded in the medial orbitofrontal cortex at the time of decision making. *Journal of Neuroscience, 30*(32), 10799-10808. doi:10.1523/JNEUROSCI.0788-10.2010

Polania, R., Krajbich, I., Grueschow, M., & Ruff, C. C. (2014). Neural oscillations and synchronization differentially support evidence accumulation in perceptual and value-based decision making. *Neuron, 82*(3), 709-720. doi:10.1016/j.neuron.2014.03.014

Polania, R., Moisa, M., Opitz, A., Grueschow, M., & Ruff, C. C. (2015). The precision of value-based choices depends causally on fronto-parietal phase coupling. *Nat Commun, 6*, 8090. doi:10.1038/ncomms9090

R Core Team. (2014). R: A language and environment for statistical computing. Vienna, Austria: R Foundation for Statistical Computing. Retrieved from http://www.R-project.org/

Rangel, A., & Hare, T. (2010). Neural computations associated with goal-directed choice. *Current opinion in neurobiology, 20*(2), 262-270. doi:https://doi.org/10.1016/j.conb.2010.03.001

Ratcliff, R., Smith, P. L., Brown, S. D., & McKoon, G. (2016). Diffusion Decision Model: Current Issues and History. *Trends Cogn Sci, 20*(4), 260-281. doi:10.1016/j.tics.2016.01.007

Schacht, A., Adler, N., Chen, P., Guo, T., & Sommer, W. (2012). Association with positive outcome induces early effects in event-related brain potentials. *Biol Psychol, 89*(1), 130-136. doi:10.1016/j.biopsycho.2011.10.001

Schulz, L., Fleming, S. M., & Dayan, P. (2021). Metacognitive Computations for Information Search: Confidence in Control. *bioRxiv*, 2021.2003.2001.433342. doi:10.1101/2021.03.01.433342

Sepulveda, P., Usher, M., Davies, N., Benson, A. A., Ortoleva, P., & De Martino, B. (2020). Visual attention modulates the integration of goal-relevant evidence and not value. *Elife, 9*, e60705. doi:10.7554/eLife.60705

Shenhav, A., & Buckner, R. L. (2014). Neural correlates of dueling affective reactions to win–win choices. *Proceedings of the National Academy of Sciences, 111*(30), 10978-10983. doi:10.1073/pnas.1405725111

Shenhav, A., Dean Wolf, C. K., & Karmarkar, U. R. (2018). The evil of banality: When choosing between the mundane feels like choosing between the worst. *J Exp Psychol Gen, 147*(12), 1892-1904. doi:10.1037/xge0000433

Shenhav, A., & Karmarkar, U. R. (2019). Dissociable components of the reward circuit are involved in appraisal versus choice. *Sci Rep, 9*(1), 1958. doi:10.1038/s41598-019-38927-7

Smith, N. J., & Kutas, M. (2015a). Regression-based estimation of ERP waveforms: I. The rERP framework. *Psychophysiology, 52*(2), 157-168. doi:10.1111/psyp.12317

Smith, N. J., & Kutas, M. (2015b). Regression-based estimation of ERP waveforms: II. Nonlinear effects, overlap correction, and practical considerations. *Psychophysiology, 52*(2), 169-181. doi:10.1111/psyp.12320

Steinemann, N. A., O'Connell, R. G., & Kelly, S. P. (2018). Decisions are expedited through multiple neural adjustments spanning the sensorimotor hierarchy. *Nat Commun, 9*(1), 3627. doi:10.1038/s41467-018-06117-0

Stine, G. M., Zylberberg, A., Ditterich, J., & Shadlen, M. N. (2020). Differentiating between integration and non-integration strategies in perceptual decision making. *eLife, 9*, e55365. doi:10.7554/eLife.55365

Strasburger, H., Rentschler, I., & Juttner, M. (2011). Peripheral vision and pattern recognition: a review. *J Vis, 11*(5), 13. doi:10.1167/11.5.13

Suess, F., & Abdel Rahman, R. (2015). Mental imagery of emotions: Electrophysiological evidence. *Neuroimage, 114*, 147-157. doi:10.1016/j.neuroimage.2015.03.063

Sun, S., Zhen, S., Fu, Z., Wu, D. A., Shimojo, S., Adolphs, R., . . . Wang, S. (2017). Decision ambiguity is mediated by a late positive potential originating from cingulate cortex. *Neuroimage, 157*, 400-414. doi:10.1016/j.neuroimage.2017.06.003

Tajima, S., Drugowitsch, J., & Pouget, A. (2016). Optimal policy for value-based decision-making. *Nat Commun, 7*(1), 12400. doi:10.1038/ncomms12400

Twomey, D. M., Murphy, P. R., Kelly, S. P., & O'Connell, R. G. (2015). The classic P300 encodes a build-to-threshold decision variable. *Eur J Neurosci, 42*(1), 1636-1643. doi:10.1111/ejn.12936

Ullsperger, M., Fischer, A. G., Nigbur, R., & Endrass, T. (2014). Neural mechanisms and temporal dynamics of performance monitoring. *Trends Cogn Sci, 18*(5), 259-267. doi:10.1016/j.tics.2014.02.009

Usher, M., & McClelland, J. L. (2001). The time course of perceptual choice: The leaky, competing accumulator model. *Psychological Review, 108*(3), 550-592. doi:10.1037/0033-295X.108.3.550

van der Meer, M., Kurth-Nelson, Z., & Redish, A. D. (2012). Information Processing in Decision-Making Systems. *The Neuroscientist, 18*(4), 342-359. doi:10.1177/1073858411435128

Wang, X. J. (2002). Probabilistic decision making by slow reverberation in cortical circuits. *Neuron, 36*(5), 955-968. doi:10.1016/s0896-6273(02)01092-9

Weichart, E. R., Turner, B. M., & Sederberg, P. B. (2020). A model of dynamic, within-trial conflict resolution for decision making. *Psychological Review, 127*(5), 749-777. doi:10.1037/rev0000191

White, J. K., Bromberg-Martin, E. S., Heilbronner, S. R., Zhang, K., Pai, J., Haber, S. N., & Monosov, I. E. (2019). A neural network for information seeking. *Nat Commun, 10*(1), 5168. doi:10.1038/s41467-019-13135-z

Wong, K. F., & Wang, X. J. (2006). A recurrent network mechanism of time integration in perceptual decisions. *Journal of Neuroscience, 26*(4), 1314-1328. doi:10.1523/JNEUROSCI.3733-05.2006

Yeung, N., & Summerfield, C. (2012). Metacognition in human decision-making: confidence and error monitoring. *Philos Trans R Soc Lond B Biol Sci, 367*(1594), 1310-1321. doi:10.1098/rstb.2011.0416